PHYSICAL REVIEW C **74**, 064002 (2006)

Scalar ΛN and $\Lambda\Lambda$ interaction in a chiral unitary approach

K. Sasaki, E. Oset, and M. J. Vicente Vacas
Departamento de Física Teórica and IFIC, Centro Mixto Universidad de Valencia—CSIC, Valencia, Spain
(Received 1 August 2006; published 13 December 2006)

We study the central part of the ΛN and $\Lambda\Lambda$ potential by considering the correlated and uncorrelated two-meson exchange in addition to the ω exchange contribution. The correlated two-meson exchange is evaluated within a chiral unitary approach. We find that a short-range repulsion is generated by the correlated two-meson potential, which also produces an attraction in the intermediate-distance region. The uncorrelated two-meson exchange produces a sizable attraction in all cases that is counterbalanced by the ω exchange contribution.

DOI: 10.1103/PhysRevC.74.064002 PACS number(s): 13.75.Ev, 12.39.Fe

I. INTRODUCTION

The scalar isoscalar potential plays an important role in the nucleon-nucleon (NN) interaction, providing an intermediate-range attraction in all channels that is demanded by the data. In models of the NN interaction using one-boson exchange (OBE) this part of the interaction was accounted for by allowing the exchange of a "σ" particle in papers as early as Ref. [1]. The exchange of a scalar particle has been a constant in other OBE models [2]. In some models a broad $\varepsilon(760)$ was advocated [3,4], and this has been used later on in more recent models [5,6]. The Particle Data Group [7] refers to the lightest scalar meson as $f_0(600)$ or σ. The nature of this particle, and even its mere existence, has been a source of controversy [8], but in recent years a strong convergence toward the idea that the σ is not a genuine meson state made up from a constituent $q\bar{q}$ pair has been witnessed [9,10]. This idea has obtained further support from unitarized chiral perturbation theory, where the σ appears as a dynamically generated resonance from the $\pi\pi$ interaction [11–19]. Other models that start from a seed of $q\bar{q}$, but couple this state to meson-meson components in a unitary approach, converge to the same idea by showing that the meson cloud is essential in building up the low-lying scalar resonances [20–22].

The picture of the σ as a dynamically generated resonance called for a new interpretation of the σ exchange in the NN interaction and this work was performed in [23]. In this work the traditional σ exchange was substituted by the exchange of two interacting mesons within the chiral unitary framework of [13], and an intermediate attraction was found together with a repulsion at short distances, which makes the picture qualitatively different from the ordinary, always attractive, σ exchange. The exchange of two interacting pions, although nonperturbative, was considered in [24] and shown to reproduce well the NN peripheral partial waves with $L > 2$. A recent work studying the isoscalar contact NN interactions retakes the unitarization of the $\pi\pi$ amplitude in the two-pion exchange using the Omnes representation [25].

The work of [23] was complemented in [26], where in addition to the interacting two-pion exchange, the contribution of the uncorrelated two-pion exchange and the repulsive contribution of the ω exchange were considered, leading altogether to a good reproduction of the empirical scalar isoscalar interaction of [27,28].

In this work we extend these ideas to the strange sector, evaluating the scalar ΛN and $\Lambda\Lambda$ interaction.

Empirical evaluations of the YN scalar-isoscalar interaction are done in several works, allowing the exchange of a scalar meson and making fits to data. As already quoted, the Nijmegen group makes use of the exchange of a heavy scalar meson and there are different fits available in the literature [5,6,29,30]. A recent work of the group shows an interesting feature—the improvement of the results by using a form factor incorporating a zero [31], which leads to qualitative features of the scalar meson exchange similar to those obtained in [23]. The exchange of various scalar mesons is also considered in [32] as well as correlated two-pion exchange, which however is treated phenomenologically. Another approach to the problem is the chiral quark model in which the π and a σ are allowed to be exchanged between constituent quarks [33,34]. Along the same line, in the works of Refs. [35,36] a SU(3) nonet of scalar mesons is exchanged between the quarks.

The closest work to our approach is the theoretical work of [37], following along the lines of the Jülich model [38, 39], where the uncorrelated and correlated two-pion exchange are considered explicitly. The approach to the correlated two-pion (and two-kaon) exchange is done rather differently by evaluating theoretically the $B\bar{B} \to \pi\pi, K\bar{K}$ amplitudes and then using unitarity and dispersion relations to relate these amplitudes to the correlated two-meson exchange contribution to the $BB \to BB$ interaction. Our approach evaluates directly the correlated two-pion exchange by explicitly using the chiral unitary approach to deal with the pion-pion interaction and using appropriate triangle diagrams to account for the coupling of the two pions to the baryons. The success of this approach in providing the scalar-isoscalar NN interaction yields solid ground for extending these ideas to the case of the ΛN and $\Lambda\Lambda$ interaction, which we present in this work.

II. CORRELATED TWO-MESON EXCHANGE BETWEEN BARYONS

We follow closely Ref. [23] and consider the correlated two-meson exchange between baryons. To evaluate these diagrams

we use the lowest order chiral Lagrangians

$$\mathcal{L}_2 = \frac{1}{6f_\pi^2}\mathrm{Tr}[\Phi\partial^\mu\Phi\Phi\partial_\mu\Phi - \Phi\Phi\partial^\mu\Phi\partial_\mu\Phi] + \frac{1}{12f_\pi^2}\mathrm{Tr}[M\Phi^4], \tag{1}$$

$$\mathcal{L}_B = \frac{D+F}{\sqrt{2}f_\pi}\mathrm{Tr}[\bar{B}\gamma_5\gamma^\mu\partial_\mu\Phi B] + \frac{D-F}{\sqrt{2}f_\pi}\mathrm{Tr}[\bar{B}\gamma_5\gamma^\mu B\partial_\mu\Phi], \tag{2}$$

where Φ and B are the standard SU(3) matrices for the octets of pseudoscalar mesons and baryons, respectively [40–46]. The mass matrix of the mesons octet is defined by $M \equiv \mathrm{diag}(m_\pi^2, m_\pi^2, 2m_K^2 - m_\pi^2)$. From there, one obtains the different pion-pion (or $K\overline{K}$) lowest order amplitudes, which can be found in [13], and the *MBB* vertices, which for convenience we show in the appendix.

The isoscalar amplitudes, which contain only the s wave, have been obtained by employing Lagrangian $\mathcal{L}_2$ in [14]. The lowest order, tree-level amplitudes of meson-meson scattering can be written as

$$t^{(I=0,L)}_{\pi\pi\to\pi\pi} = -\frac{1}{f_\pi^2}\left(s - \frac{m_\pi^2}{2}\right) + \frac{1}{3f_\pi^2}\sum_i (p_i^2 - m_i^2), \tag{3}$$

$$t^{(I=0,L)}_{K\overline{K}\to K\overline{K}} = -\frac{3s}{4f_\pi^2} + \frac{1}{4f_\pi^2}\sum_i (p_i^2 - m_i^2), \tag{4}$$

$$t^{(I=0,L)}_{\pi\pi\to K\overline{K}} = -\frac{\sqrt{3}s}{4f_\pi^2} + \frac{1}{4\sqrt{3}f_\pi^2}\sum_i (p_i^2 - m_i^2), \tag{5}$$

where the superscript L stands for the leading-order amplitude of meson-meson scattering and we have employed the convenient unitary normalization and the isospin phase convention ($|\pi^+\rangle = -|1,1\rangle$, $|K^-\rangle = -|1/2,-1/2\rangle$):

$$|\pi\pi, (I=0)\rangle = -\frac{1}{\sqrt{6}}|\pi^0\pi^0 + \pi^+\pi^- + \pi^-\pi^+\rangle, \tag{6}$$

$$|K\overline{K}(I=0)\rangle = -\frac{1}{\sqrt{2}}|K^0\overline{K}^0 + K^+K^-\rangle. \tag{7}$$

In Eqs. (3)–(5) we have separated the lowest order interaction into a part, which provides the on-shell contribution, and another term [the one with $(p_i^2 - m_i^2)$], which contributes only for off-shell mesons.

As shown in [14,23,26], the off-shell part of the meson-meson amplitudes does not contribute to our calculation. In fact, for the meson-meson loops, this contribution is absorbed into the physical mass and the coupling. As for the coupling to the baryons, there is a cancelation of the off-shell part of the meson-meson amplitude in Eqs. (3)–(5) with the diagrams of the type of Fig. 1. This fact is valid not only for the *NN*

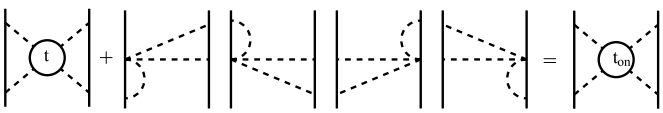

FIG. 1. Set of diagrams that cancel the of-shell part of the correlated two-meson exchange contribution.

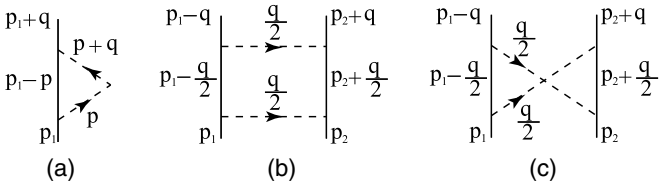

FIG. 2. Diagrams explicitly showing the momentum assignment. In our calculation we take the static limit for the initial baryons.

case but also for the *YN* and *YY* cases. Thus, hereafter, we only consider the on-shell part of the meson-meson amplitude.

This on-shell treatment enables us to separate the on-shell meson-meson amplitude from the triangle loop integration that couples the mesons to the baryons. Thus we can define the correlated two-meson potential as

$$V^{\mathrm{Cor}}_{B_1B_2}(q) = \sum_{ij}^{\pi\pi,K\overline{K}} N_{ij}\Delta^i_{B_1}t^{(I=0,L)}_{i\to j}\Delta^j_{B_2}, \tag{8}$$

where Δ indicates the triangle loop contribution of the two-meson potential for baryon B_k and N_{ij} is a factor from the isospin summation ($N_{\pi\pi,\pi\pi} = 6$, $N_{\pi\pi,K\overline{K}} = N_{K\overline{K},\pi\pi} = 2\sqrt{3}$, and $N_{K\overline{K},K\overline{K}} = 2$). For concreteness, the Δ function in the correlated two-pion potential for the *NN* channel is given by

$$\Delta^{(\pi\pi)}_N = \left(\frac{D+F}{2f_\pi}\right)^2 V^{(\pi\pi)}_{NN}(q), \tag{9}$$

where $V^{(m_1m_2)}_{B'B}(q)$ is the vertex function with intermediate baryon B' which is already evaluated in [23] and given in a generalized form as

$$V^{(m_1m_2)}_{B'B}(q) = \int \frac{d^3p}{(2\pi)^3}\frac{M_{B'}}{E_{B'}(\vec{p})}\frac{(\vec{p}+\vec{q})\cdot\vec{p}}{2\omega_1\omega_2(\omega_1+\omega_2)} \times \frac{\omega_1+\omega_2+E_{B'}(\vec{p})-M_B}{(\omega_1+E_{B'}(\vec{p})-M_B)(\omega_2+E_{B'}(\vec{p})-M_B)}, \tag{10}$$

with

$$E_{B'}(\vec{p}) = \sqrt{\vec{p}^2 + M_{B'}^2}, \quad \omega_1 = \sqrt{\mu_1^2 + \vec{p}^2}, \quad \omega_2 = \sqrt{\mu_2^2 + (\vec{p}+\vec{q})^2}. \tag{11}$$

This is calculated with the variables corresponding to Fig. 2(a) and where, as in [23], we have used the initial momentum at rest. We introduce a static form factor to regularize the triangle loop function. The form factor employed in this calculation is

$$F(\vec{p})F(\vec{p}+\vec{q}) = \frac{\Lambda^2}{\Lambda^2+\vec{p}^2}\frac{\Lambda^2}{\Lambda^2+(\vec{p}+\vec{q})^2}, \tag{12}$$

where the cutoff is chosen as $\Lambda = 1.0$ GeV.

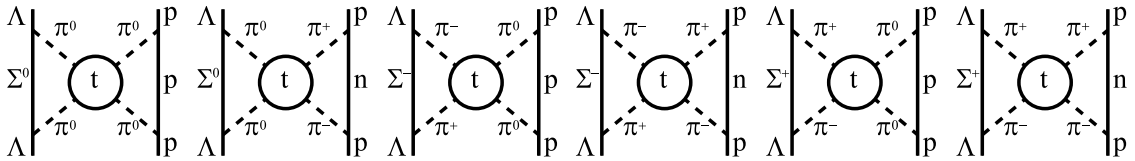

FIG. 3. Diagrams of scalar-isoscalar ΛN processes involving $t_{\pi\pi\to\pi\pi}$.

A. Lowest order contribution in the isoscalar exchange in the $\Lambda N \to \Lambda N$ interaction

For this case the potential generated by the correlated two-pion diagrams shown in Fig. 3 is given by

$$V^{\pi\pi\to\pi\pi} = 6\left[\left(\frac{D}{\sqrt{3}f_\pi}\right)^2 V_{\Sigma\Lambda}^{(\pi\pi)}(q)\right] t_{\pi\pi\to\pi\pi}^{(I=0,L)} \times \left[\left(\frac{D+F}{2f_\pi}\right)^2 V_{NN}^{(\pi\pi)}(q)\right], \tag{13}$$

where $V_{\Sigma\Lambda}^{(\pi\pi)}(q)$ is the vertex function defined in Eq. (10) with the same form factor. Furthermore, as described in Sec. II C, we substitute $t_{\pi\pi\to\pi\pi}^{(I=0,L)}$ by the full unitarized amplitude. From now on we consider directly the full meson-meson amplitudes in all cases.

We also include the exchange of $K\overline{K}$ in the approach. The diagrams to take into account are shown in Fig. 4. By using the couplings in the appendix, we evaluate the potential generated by the correlated $K\overline{K}$ contributions in a similar way as before, obtaining

$$V^{K\overline{K}\to K\overline{K}} = 2\Delta_\Lambda^{K\overline{K}} t_{K\overline{K}\to K\overline{K}}^{(I=0,L)} \Delta_N^{K\overline{K}}, \tag{14}$$

with the triangle kaon-loop contribution given by

$$\Delta_\Lambda^{(K\overline{K})} = \left(\frac{D+3F}{2\sqrt{3}f_\pi}\right)^2 V_{N\Lambda}^{(K\overline{K})}(q) + \left(\frac{3F-D}{2\sqrt{3}f_\pi}\right)^2 V_{\Xi\Lambda}^{(K\overline{K})}(q), \tag{15}$$

$$\Delta_N^{(K\overline{K})} = \frac{3}{2}\left(\frac{D-F}{2\sqrt{3}f_\pi}\right)^2 V_{\Sigma N}^{(K\overline{K})}(q) + \frac{1}{2}\left(\frac{D+3F}{2\sqrt{3}f_\pi}\right)^2 V_{\Lambda N}^{(K\overline{K})}(q). \tag{16}$$

The factors in front of the parentheses for $\Delta_N^{(K\overline{K})}$ come from the $I=0$ projection of the kaon couplings.

Now one must consider the mixed terms for vertices with π or K that involve the $\pi\pi \to K\overline{K}$ transition amplitude. The diagrams to consider are shown in Fig. 5. The potential in this case is given by

$$V^{\pi\pi\to K\overline{K}} = 2\sqrt{3}\Delta_\Lambda^{\pi\pi} t_{\pi\pi\to K\overline{K}}^{(I=0,L)} \Delta_N^{K\overline{K}} + 2\sqrt{3}\Delta_\Lambda^{K\overline{K}} t_{K\overline{K}\to\pi\pi}^{(I=0,L)} \Delta_N^{\pi\pi}, \tag{17}$$

with the triangle meson-loop contribution shown before.

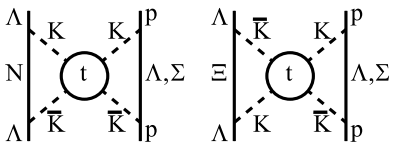

FIG. 4. Diagrams involving $t_{K\overline{K}\to K\overline{K}}$.

B. Contribution of Δ, Σ^*, and Ξ^* intermediate states

Next we wish to include the contribution of the intermediate Δ, Σ^*, and Ξ^* states. In the block of diagrams of Fig. 3 we can introduce Σ^* in the left triangular vertex, or Δ in the right triangular vertex, or both.

The coupling of the decuplet to the octet of mesons and baryons is given by

$$\mathcal{L}^{\rm Dec} = \frac{\sqrt{2}}{f_\pi}\mathcal{C}\sum_{a,b,c,d,e}^{1\sim3} \epsilon^{abc}\left(\left(\bar{T}_{ade}\Phi_b^d B_c^e\right)\vec{S}\cdot(-\vec{q}) + \left(\bar{B}_e^c \Phi_d^b T_{ade}\right)\vec{S}^\dagger\cdot\vec{q}\right) \tag{18}$$

for an outgoing meson with momentum q. The $\mathcal{C}$ is determined from the $\Delta N\pi$ coupling constant. T is the decuplet baryon field shown in the appendix. This Lagrangian gives rise to couplings of the type

$$\gamma_{MBB'}\frac{f^*_{\pi N\Delta}}{m_\pi}\vec{S}\cdot\vec{q} \tag{19}$$

for outgoing mesons of momentum $\vec{q}$. The $\gamma_{MBB'}$ coefficients can be found in the appendix. We use $f^*_{\pi N\Delta} = 2.12 f_{\pi NN}$ to obtain the correct width of the $\Delta(1232)$ resonance.

Altogether, the contribution involving the $\pi\pi \to \pi\pi$ amplitude is given by

$$V^{(\pi\pi\to\pi\pi)} = 6t_{\pi\pi\to\pi\pi}^{(I=0,L)}\left[\left(\frac{D}{\sqrt{3}f_\pi}\right)^2 V_{\Sigma\Lambda}^{(\pi\pi)}(q) + \frac{2}{3}\left(\frac{f^*_{\pi N\Delta}}{\sqrt{2}m_\pi}\right)^2 V_{\Sigma^* N}^{(\pi\pi)}(q)\right] \times \left[\left(\frac{D+F}{2f_\pi}\right)^2 V_{N\Lambda}^{(\pi\pi)}(q) + \frac{4}{9}\left(\frac{f^*_{\pi N\Delta}}{m_\pi}\right)^2 V_{\Delta N}^{(\pi\pi)}(q)\right], \tag{20}$$

where the factor 2/3 comes from the difference of spin and the extra 2/3 in front of $V_{\Delta N}^{(\pi\pi)}$ from the change of isospin. This equation shows how the triangle loop contribution is modified by the excited baryon in the intermediate state.

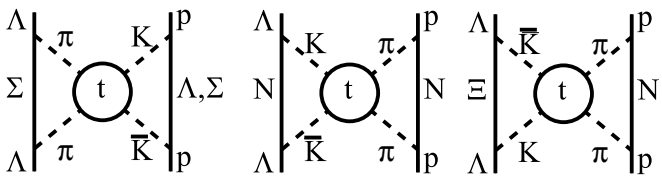

FIG. 5. Diagrams involving $t_{\pi\pi\to K\overline{K}}$.

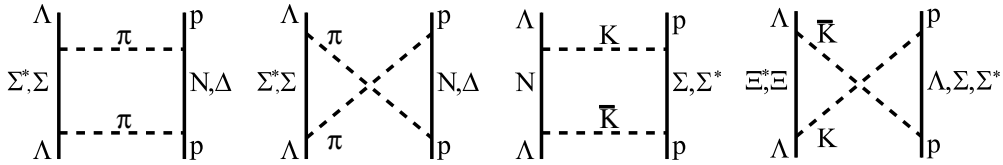

FIG. 6. Uncorrelated two-pion and two-kaon diagrams.

Thus, the modified triangle loop contribution can be written as

$$\tilde{\Delta}_{\Lambda}^{(\pi\pi)} = \Delta_{\Lambda}^{(\pi\pi)} + \frac{2}{3}\left(\frac{f^*_{\pi N\Delta}}{\sqrt{2}m_\pi}\right)^2 V^{(\pi\pi)}_{\Sigma^* N}(q), \tag{21}$$

$$\tilde{\Delta}_{N}^{(\pi\pi)} = \Delta_{N}^{(\pi\pi)} + \frac{4}{9}\left(\frac{f^*_{\pi N\Delta}}{m_\pi}\right)^2 V^{(\pi\pi)}_{\Delta N}(q). \tag{22}$$

In the same way we take into account the contributions of Σ^*, Ξ^* in the $K\overline{K}$ triangle contribution by means of the couplings of the appendix, and the results are given by

$$\tilde{\Delta}_{\Lambda}^{(K\overline{K})} = \Delta_{\Lambda}^{(K\overline{K})} + \frac{2}{3}\left(\frac{f^*_{\pi N\Delta}}{\sqrt{2}m_\pi}\right)^2 V^{K\bar{K}}_{\Xi^*}(q), \tag{23}$$

$$\tilde{\Delta}_{N}^{(K\overline{K})} = \Delta_{N}^{(K\overline{K})} + \frac{2}{3}\left(\frac{f^*_{\pi N\Delta}}{\sqrt{6}m_\pi}\right)^2 V^{K\bar{K}}_{\Sigma^*}(q). \tag{24}$$

Therefore the total leading-order potential generated by the correlated two-meson contribution with the excited baryons in the intermediate states is given by substitution of the Δ to the $\tilde{\Delta}$ as

$$V^{\rm Cor}_{\Lambda N}(q) = \sum_{i,j}^{\pi\pi, K\overline{K}} N_{ij}\,\tilde{\Delta}^i_{\Lambda}\, t^{(I=0,L)}_{i\to j}\,\tilde{\Delta}^j_{N}. \tag{25}$$

C. Unitarization of the amplitudes

Here we follow Ref. [13] and iterate the meson-meson potential to infinite order by using a Lippmann-Schwinger-type equation in coupled $\pi\pi$ and $K\overline{K}$ channels. As shown in [13,14], the Lippmann-Schwinger equation can be reduced under the on-shell factorization to the algebraic relation

$$T = [1 - VG]^{-1} V, \tag{26}$$

where $V \equiv t$ used in the former Eqs. (3)–(5), and G is the meson-meson loop function. The G function is given by

$$G(s) = \int_0^{q_{\rm max}} \frac{q^2 dq}{(2\pi)^2} \frac{\omega_1 + \omega_2}{\omega_1\omega_2[s - (\omega_1+\omega_2)^2 + i\epsilon]}, \tag{27}$$

where $\omega_i = \sqrt{\vec{q}^2 + m_i^2}$. It is regularized with a cutoff scheme, which is different from the expression used in the previous paper [23]. One advantage of the usage of a cutoff is that it does not produce undesirable poles as mentioned in [23]. For the region of interest to us, one can use both cutoff or dimensional regularization to evaluate G. Some caveats about the use at unreasonably low negative values of s are discussed in [23], which set restrictions on the results at very short distances.

We have also included the $\eta\eta$ channel but their effect is small and can be approximately reabsorbed in the $\pi\pi$, $K\overline{K}$ channels by redefining $q_{\rm max}$ [16]. We obtain good results for the $\pi\pi$ phase shift up to 1.2 GeV by using the $\pi\pi$, $K\overline{K}$ channels and $q_{\rm max} = 1.0$ GeV.

The final expression for the correlated two-meson ΛN scalar potential is given by summing the expressions in Eq. (25) and substituting t_i by the unitarized amplitude T_i.

III. UNCORRELATED TWO-MESON EXCHANGE

We consider both the direct and crossed diagrams of the uncorrelated two-pion and two-kaon exchange contributions shown in Fig. 6. We follow here the procedure of [26] and use the variables of the diagrams as shown in Figs. 2(b) and 2(c).

After performing analytically the p^0 integration we obtain the uncorrelated two-meson potential in terms of the integrals

$$V^{(i,m_1m_2)}_{B_1B_2}(q) = -\int \frac{d^3p}{(2\pi)^3}\frac{M_1}{E_1}\frac{M_2}{E_2}\left(p^2 - \frac{q^2}{4}\right)^2 R_i(\cdot), \tag{28}$$

where M_1 and M_2 are the intermediate baryon masses, i stands for the direct (D) or crossed (C) terms, and

$$R_D(\cdot) = \frac{(\omega_1+\omega_2)((E'_1+E'_2)^2 + 2\omega_1\omega_2) + (\omega_1^2 + 3\omega_1\omega_2 + \omega_2^2 + E'_1E'_2)(E'_1+E'_2)}{2\omega_1\omega_2(\omega_1+\omega_2)(E'_1+E'_2)(\omega_1+E'_1)(\omega_1+E'_2)(\omega_2+E'_1)(\omega_2+E'_2)}, \tag{29}$$

$$R_C(\cdot) = \frac{(\omega_1+\omega_2)(E'_1+E'_2) + \omega_1^2 + \omega_1\omega_2 + \omega_2^2 + E'_1E'_2}{2\omega_1\omega_2(\omega_1+\omega_2)(\omega_1+E'_1)(\omega_1+E'_2)(\omega_2+E'_1)(\omega_2+E'_2)}, \tag{30}$$

with $E'_i = E_i - p^0_I$. It is worth mentioning that, if we compare to results without coupling constants, the crossed contribution is much smaller than the box-type contribution. Furthermore, both V^D and V^C are largely suppressed by the mass of the exchanged meson. As a result of this rough estimation, we expect that the uncorrelated two-kaon contribution is much smaller than the uncorrelated two-pion contribution.

By taking the coupling of the vertices in the different diagrams into account we get the contribution to the ΛN

potential by considering the contribution of the Δ, Σ^*, Ξ^* in the intermediate states as

$$
\begin{aligned}
v_{\Lambda N}^{(D,\pi\pi)} &= 3\left(\frac{D}{\sqrt{3}f_\pi}\right)^2\left(\frac{D+F}{2f_\pi}\right)^2 V_{\Sigma N}^{(D,\pi\pi)}(q) \\
&+2\left(\frac{D+F}{2f_\pi}\right)^2\left(\frac{f^*_{\pi N\Delta}}{\sqrt{2}m_\pi}\right)^2 V_{\Sigma^* N}^{(D,\pi\pi)}(q) \\
&+\frac{4}{3}\left(\frac{D}{\sqrt{3}f_\pi}\right)^2\left(\frac{f^*_{\pi N\Delta}}{m_\pi}\right)^2 V_{\Sigma\Delta}^{(D,\pi\pi)}(q) \\
&+\frac{8}{9}\left(\frac{f^*_{\pi N\Delta}}{\sqrt{2}m_\pi}\right)^2\left(\frac{f^*_{\pi N\Delta}}{m_\pi}\right)^2 V_{\Sigma^*\Delta}^{(D,\pi\pi)}(q), \\
v_{\Lambda N}^{(C,\pi\pi)} &= 3\left(\frac{D}{\sqrt{3}f_\pi}\right)^2\left(\frac{D+F}{2f_\pi}\right)^2 V_{\Sigma N}^{(C,\pi\pi)}(q) \\
&+2\left(\frac{f^*_{\pi N\Delta}}{\sqrt{2}m_\pi}\right)^2\left(\frac{D+F}{2f_\pi}\right)^2 V_{\Sigma^* N}^{(C,\pi\pi)}(q) \\
&+\frac{4}{3}\left(\frac{D}{\sqrt{3}f_\pi}\right)^2\left(\frac{f^*_{\pi N\Delta}}{m_\pi}\right)^2 V_{\Sigma\Delta}^{(C,\pi\pi)}(q) \\
&+\frac{8}{9}\left(\frac{f^*_{\pi N\Delta}}{\sqrt{2}m_\pi}\right)^2\left(\frac{f^*_{\pi N\Delta}}{m_\pi}\right)^2 V_{\Sigma^*\Delta}^{(C,\pi\pi)}(q),
\end{aligned}
\tag{31}
$$

where we write explicitly the left and right baryon in the diagrams and the couple of mesons exchanged.

Similarly, for the $K\overline{K}$ diagrams we calculate the uncorrelated two-kaon potential as

$$
\begin{aligned}
v_{\Lambda N}^{(D,K\overline{K})} &= 3\left(\frac{D+3F}{2\sqrt{3}f_\pi}\right)^2\left(\frac{D-F}{2f_\pi}\right)^2 V_{N\Sigma}^{(D,K\overline{K})}(q) \\
&+\frac{1}{3}\left(\frac{D+3F}{2\sqrt{3}f_\pi}\right)^2\left(\frac{f^*_{\pi N\Delta}}{m_\pi}\right)^2 V_{N\Sigma^*}^{(D,K\overline{K})}(q), \\
v_{\Lambda N}^{(C,K\overline{K})} &= 3\left(\frac{3F-D}{2\sqrt{3}f_\pi}\right)^2\left(\frac{D-F}{2f_\pi}\right)^2 V_{\Xi\Sigma}^{(C,\overline{K}K)}(q) \\
&+2\left(\frac{f^*_{\pi N\Delta}}{\sqrt{2}m_\pi}\right)^2\left(\frac{D-F}{2f_\pi}\right)^2 V_{\Xi^*\Sigma}^{(C,\overline{K}K)}(q) \\
&+2\left(\frac{3F-D}{2\sqrt{3}f_\pi}\right)^2\left(\frac{f^*_{\pi N\Delta}}{\sqrt{6}m_\pi}\right)^2 V_{\Xi\Sigma^*}^{(C,\overline{K}K)}(q) \\
&+\frac{4}{3}\left(\frac{f^*_{\pi N\Delta}}{\sqrt{2}m_\pi}\right)^2\left(\frac{f^*_{\pi N\Delta}}{\sqrt{6}m_\pi}\right)^2 V_{\Xi^*\Sigma^*}^{(C,\overline{K}K)}(q) \\
&+\left(\frac{3F-D}{2\sqrt{3}f_\pi}\right)^2\left(\frac{3F+D}{2\sqrt{3}f_\pi}\right)^2 V_{\Xi\Lambda}^{(C,\overline{K}K)}(q) \\
&+\frac{2}{3}\left(\frac{f^*_{\pi N\Delta}}{\sqrt{2}m_\pi}\right)^2\left(\frac{3F+D}{2\sqrt{3}f_\pi}\right)^2 V_{\Xi^*\Lambda}^{(C,\overline{K}K)}(q).
\end{aligned}
\tag{32}
$$

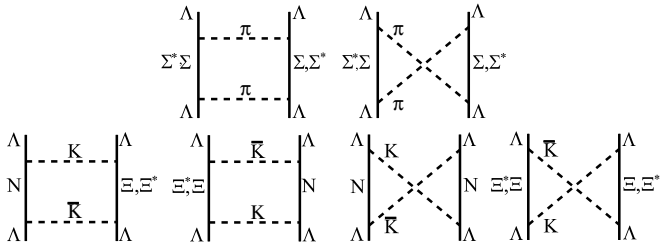

FIG. 7. Set of the uncorrelated two-meson exchange diagrams for the $\Lambda\Lambda$ interaction.

In this case the $K\overline{K}$ crossed diagrams have more variety than for the $\pi\pi$ case, but the potential does not change as much because the contribution of $V^{(C,K\overline{K})}$ is quite small, as previously explained.

IV. THE ω EXCHANGE CONTRIBUTION

Here we take into account the ω exchange potential, which is known to be one of main sources of short-range repulsion of the baryon-baryon interaction. The ω exchange potential for ΛN in momentum space is given by

$$
V_{\Lambda N}^{\omega}(q) = \frac{g_{\omega\Lambda\Lambda}g_{\omega NN}}{q^2+m_\omega^2}\left(\frac{\Lambda_\omega^2-m_\omega^2}{\Lambda_\omega^2+q^2}\right)^2, \tag{33}
$$

where we choose $g_{\omega NN}=13$ and $\Lambda_\omega = 1.4$ GeV [26]. The ideal mixing for ω and ϕ leads to the relation $g_{\omega\Lambda\Lambda}=\frac{2}{3}g_{\omega NN}$, which is deduced from the quark contents of the hadrons. For simplicity we assume the same form factor for both the ωNN and $\omega\Lambda\Lambda$ vertices.

V. THE ISOSCALAR EXCHANGE IN THE $\Lambda\Lambda$ INTERACTION

We easily extend this method to the $\Lambda\Lambda$ interaction. For this we simply replace the triangle contribution of the nucleon by that of the Λ in Eq. (25):

$$
V_{\Lambda\Lambda}^{\mathrm{Cor}}(q) = \sum_{i,j}^{\pi\pi,K\overline{K}} N_{ij}\,\tilde{\Delta}_\Lambda^i\, t_{i\to j}^{(I=0,L)}\,\tilde{\Delta}_\Lambda^j, \tag{34}
$$

where all contributions are as shown before.

The uncorrelated two-meson exchange potential is given by

$$
\begin{aligned}
v_{\Lambda\Lambda}^{(D,\pi\pi)} &= 3\left(\frac{D}{\sqrt{3}f_\pi}\right)^4 V_{\Sigma\Sigma}^{(D,\pi\pi)}(q) \\
&+3\left(\frac{f^*_{\pi N\Delta}}{\sqrt{2}m_\pi}\right)^2\left(\frac{D}{\sqrt{3}f_\pi}\right)^2 V_{\Sigma^*\Sigma}^{(D,\pi\pi)}(q) \\
&+3\left(\frac{D}{\sqrt{3}f_\pi}\right)^2\left(\frac{f^*_{\pi N\Delta}}{\sqrt{2}m_\pi}\right)^2 V_{\Sigma\Sigma^*}^{(D,\pi\pi)}(q) \\
&+3\left(\frac{f^*_{\pi N\Delta}}{\sqrt{2}m_\pi}\right)^4 V_{\Sigma^*\Sigma^*}^{(D,\pi\pi)}(q),
\end{aligned}
$$

$$
\begin{aligned}
v_{\Lambda\Lambda}^{(C,\pi\pi)} &= 3\left(\frac{D}{\sqrt{3}f_\pi}\right)^4 V_{\Sigma\Sigma}^{(C,\pi\pi)}(q) \\
&+3\left(\frac{f^*_{\pi N\Delta}}{\sqrt{2}m_\pi}\right)^2\left(\frac{D}{\sqrt{3}f_\pi}\right)^2 V_{\Sigma^*\Sigma}^{(C,\pi\pi)}(q) \\
&+3\left(\frac{D}{\sqrt{3}f_\pi}\right)^2\left(\frac{f^*_{\pi N\Delta}}{\sqrt{2}m_\pi}\right)^2 V_{\Sigma\Sigma^*}^{(C,\pi\pi)}(q) \\
&+3\left(\frac{f^*_{\pi N\Delta}}{\sqrt{2}m_\pi}\right)^4 V_{\Sigma^*\Sigma^*}^{(C,\pi\pi)}(q).
\end{aligned}
\tag{35}
$$

The two-kaon exchange is given by

$$
\begin{aligned}
v_{\Lambda\Lambda}^{(D,K\overline{K})} &= 2\left(\frac{3F-D}{2\sqrt{3}f_\pi}\right)^2\left(\frac{D+3F}{2\sqrt{3}f_\pi}\right)^2 V_{\Xi N}^{(D,K\overline{K})}(q) \\
&+2\left(\frac{f^*_{\pi N\Delta}}{\sqrt{2}m_\pi}\right)^2\left(\frac{D+3F}{2\sqrt{3}f_\pi}\right)^2 V_{\Xi^* N}^{(D,K\overline{K})}(q) \\
&+2\left(\frac{D+3F}{2\sqrt{3}f_\pi}\right)^2\left(\frac{3F-D}{2\sqrt{3}f_\pi}\right)^2 V_{N\Xi}^{(D,\overline{K}K)}(q) \\
&+2\left(\frac{D+3F}{2\sqrt{3}f_\pi}\right)^2\left(\frac{f^*_{\pi N\Delta}}{\sqrt{2}m_\pi}\right)^2 V_{N\Xi^*}^{(D,\overline{K}K)}(q),
\end{aligned}
\tag{36}
$$

$$
\begin{aligned}
v_{\Lambda\Lambda}^{(C,K\overline{K})} &= 2\left(\frac{3F-D}{2\sqrt{3}f_\pi}\right)^4 V_{\Xi\Xi}^{(C,K\overline{K})}(q) \\
&+2\left(\frac{f^*_{\pi N\Delta}}{\sqrt{2}m_\pi}\right)^2\left(\frac{3F-D}{2\sqrt{3}f_\pi}\right)^2 V_{\Xi^*\Xi}^{(C,K\overline{K})}(q) \\
&+2\left(\frac{3F-D}{2\sqrt{3}f_\pi}\right)^2\left(\frac{f^*_{\pi N\Delta}}{\sqrt{2}m_\pi}\right)^2 V_{\Xi\Xi^*}^{(C,K\overline{K})}(q) \\
&+2\left(\frac{f^*_{\pi N\Delta}}{\sqrt{2}m_\pi}\right)^4 V_{\Xi^*\Xi^*}^{(C,K\overline{K})}(q) \\
&+2\left(\frac{D+3F}{2\sqrt{3}f_\pi}\right)^4 V_{NN}^{(C,\overline{K}K)}(q).
\end{aligned}
$$

The ω exchange potential is also considered by substituting $g_{\omega NN}$ to $g_{\omega\Lambda\Lambda}$ in Eq. (33). The corresponding diagrams are shown in Fig. 7.

VI. SCALAR πK EXCHANGE IN THE κ CHANNEL

In the interactions of the octet of mesons in the πK channel one also finds a very broad resonance [14]—the κ with $S=-1$, $I=1/2$, and $J^P=0^+$, around 800 MeV, although this identification is somewhat controversial [47–51]. Its exchange is also accounted for in the recent model of [37].

Here we follow the same approach as in the former section and exchange πK in the $I=1/2, l=0$ channel. For this we consider the diagrams of Fig. 8. By following the same rules as before we find for the sum of all diagrams the compact

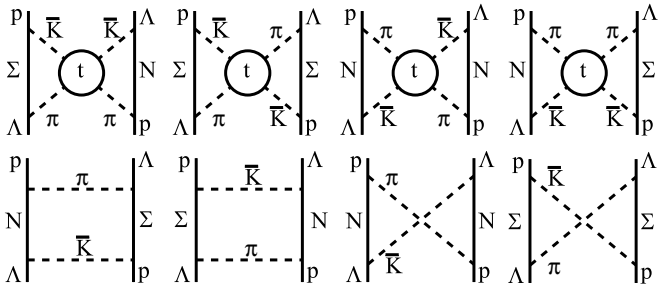

FIG. 8. Set of diagrams that contribute to the κ channel.

expression

$$
\begin{aligned}
&3t_{\pi\overline{K}\to\pi\overline{K}}^{(I=1/2,L)}\left\{-\left(\frac{D+3F}{2\sqrt{3}f_\pi}\right)\left(\frac{D+F}{2f_\pi}\right)V_N^{(\pi K)}(q)\right. \\
&\left.+\left(\frac{D}{\sqrt{3}f_\pi}\right)\left(\frac{D-F}{2f_\pi}\right)V_\Sigma^{(\pi K)}(q)\right\}^2,
\end{aligned}
\tag{37}
$$

which, including the contribution of the Σ^* states (since there are no Δ or Ξ^* intermediate states now), gives

$$
\begin{aligned}
&3t_{\pi\overline{K}\to\pi\overline{K}}^{(I=1/2,L)}\left\{-\left(\frac{D+3F}{2\sqrt{3}f_\pi}\right)\left(\frac{D+F}{2f_\pi}\right)V_N^{(\pi K)}(q)\right. \\
&+\left(\frac{D}{\sqrt{3}f_\pi}\right)\left(\frac{D-F}{2f_\pi}\right)V_\Sigma^{(\pi K)}(q) \\
&\left.-\frac{2}{3}\left(\frac{f^*_{\pi N\Delta}}{\sqrt{6}m_\pi}\right)\left(\frac{f^*_{\pi N\Delta}}{\sqrt{2}m_\pi}\right)V_{\Sigma^*}^{(\pi K)}(q)\right\}^2.
\end{aligned}
\tag{38}
$$

The $\pi\overline{K}\to\pi\overline{K}$ amplitude in the $I=1/2$ channel can be obtained from the appendix of [14] and we have

$$
t_{\pi\overline{K}\to\pi\overline{K}}^{(I=1/2,L)} = \frac{1}{4f_\pi^2}\left(3u-s-2m_\pi^2-2m_K^2\right),
\tag{39}
$$

which after projection over $l=0$ gives [52]

$$
t_{\pi\overline{K}\to\pi\overline{K}}^{(I=1/2,L)}(l=0) = \frac{1}{4f_\pi^2}\left(-\frac{5}{2}s+m_\pi^2+m_K^2+\frac{3\left(m_K^2-m_\pi^2\right)^2}{2s}\right).
\tag{40}
$$

To avoid the singular behavior around $s=0$, we take the $SU(3)_f$ limit in the $\pi\overline{K}$ amplitude. Then we can obtain the modified $\pi\overline{K}\to\pi\overline{K}$ amplitude as

$$
t_{\pi\overline{K}\to\pi\overline{K}}^{(I=1/2,L)}(l=0) = \frac{1}{4f_\pi^2}\left(-\frac{5}{2}s+2m'^2\right),
\tag{41}
$$

where m' is the average mass of the pion and the kaon. This amplitude is also unitarized in the same way as before with only one channel.

Next we calculate the uncorrelated πK diagrams shown in Fig. 8 by considering the decuplet excitation of the intermediate baryon. These diagrams give

$$
\begin{aligned}
v_{\Lambda N(\kappa)}^{(D,\pi K)} &= -3\left(\frac{D+F}{2f_\pi}\right)\left(\frac{D+3F}{2\sqrt{3}f_\pi}\right)\left(\frac{D}{\sqrt{3}f_\pi}\right) \\
&\times\left(\frac{D-F}{2f_\pi}\right)V_{N\Sigma}^{(D,\pi K)}(q)+\frac{1}{\sqrt{3}}\left(\frac{D+F}{2f_\pi}\right)
\end{aligned}
$$

$$\times \left(\frac{D+3F}{2\sqrt{3}f_\pi}\right)\left(\frac{f^*_{\pi N\Delta}}{m_\pi}\right)^2 V^{(D,\pi K)}_{N\Sigma^*}(q),$$

$$v^{(D,K\pi)}_{\Lambda N(\kappa)} = -3\left(\frac{D+F}{2f_\pi}\right)\left(\frac{D}{\sqrt{3}f_\pi}\right)\left(\frac{D+3F}{2\sqrt{3}f_\pi}\right) \times \left(\frac{D-F}{2f_\pi}\right) V^{(D,K\pi)}_{\Sigma N}(q) + \frac{1}{\sqrt{3}}\left(\frac{D+F}{2f_\pi}\right) \times \left(\frac{D+3F}{2\sqrt{3}f_\pi}\right)\left(\frac{f^*_{\pi N\Delta}}{m_\pi}\right)^2 V^{(D,K\pi)}_{\Sigma^* N}(q),$$

$$v^{(C,\pi K)}_{\Lambda N(\kappa)} = 3\left(\frac{D+F}{2f_\pi}\right)^2\left(\frac{D+3F}{2\sqrt{3}f_\pi}\right)^2 V^{(C,\pi K)}_{NN}(q),$$

$$v^{(C,K\pi)}_{\Lambda N(\kappa)} = 3\left(\frac{D}{\sqrt{3}f_\pi}\right)^2\left(\frac{D-F}{2f_\pi}\right)^2 V^{(C,K\pi)}_{\Sigma\Sigma}(q) - \frac{1}{\sqrt{3}}\left(\frac{D}{\sqrt{3}f_\pi}\right)\left(\frac{D-F}{2f_\pi}\right)\left(\frac{f^*_{\pi N\Delta}}{m_\pi}\right)^2 V^{(C,K\pi)}_{\Sigma\Sigma^*}(q) - \frac{1}{\sqrt{3}}\left(\frac{D}{\sqrt{3}f_\pi}\right)\left(\frac{D-F}{2f_\pi}\right)\left(\frac{f^*_{\pi N\Delta}}{m_\pi}\right)^2 V^{(C,K\pi)}_{\Sigma^*\Sigma}(q) + \frac{1}{9}\left(\frac{f^*_{\pi N\Delta}}{m_\pi}\right)^4 V^{(C,K\pi)}_{\Sigma^*\Sigma^*}(q), \quad (42)$$

where we follow this prescription for the meson pair of the superindex: The first meson corresponds to the upper one in the direct exchange and to the upper one on the left baryon for the crossed terms.

VII. RESULTS

A. ΛN potential in momentum space

Figure 9 shows the ΛN potential in momentum space. The correlated two-meson contribution has a peak around $q = 400$ MeV. A similar peak in position and magnitude was found for the NN case in Refs. [23,26,53]. It is worth discussing this shape because it is impossible to parameterize it by a single-meson exchange with usual form factors, such as monopole or Gaussian. This contribution could be decomposed in, at least, two parts, one a strong repulsive part and the other a weak attraction. In any case, this contribution is much smaller than the other ones, so that the main contribution comes from the uncorrelated two-meson exchange and from ω exchange. These two potentials have opposite sign, and the uncorrelated two-meson potential is slightly stronger than the ω exchange potential in the whole range of q. Thus, the sum of these two potentials is always negative.

The total potential has positive strength around $q =$ 600 MeV, which is pushed up by the correlated two-meson potential. The correlated two-meson potential plays a more important role in this region.

We can see the relevance of the two-kaon contribution to this potential by comparing the left and right panels in Fig. 9. The two-kaon contribution was studied since one-kaon exchange is important in the ΛN interaction. However, the effect of the two-kaon contribution, which is suppressed because of its heavy mass, is very small and does not significantly alter the pionic potential.

B. ΛN potential in configuration space

The ΛN potential in configuration space (shown in Fig. 10) is given by

$$V(r) = \frac{1}{2\pi^2 r}\int_0^\infty q\,\sin(qr)V(q)dq. \quad (43)$$

In the left panel of this figure, we can see a correlated two-pion potential similar to the NN case (see Fig. 10 in [23]). This should be expected since the definition of the potential is quite similar to the NN case except for the masses of the baryons and coupling constants. In fact both the NN and ΛN potentials generated by the correlated two-pion exchange contribution pass through zero at $r \simeq 0.9$ fm and have a minimum at

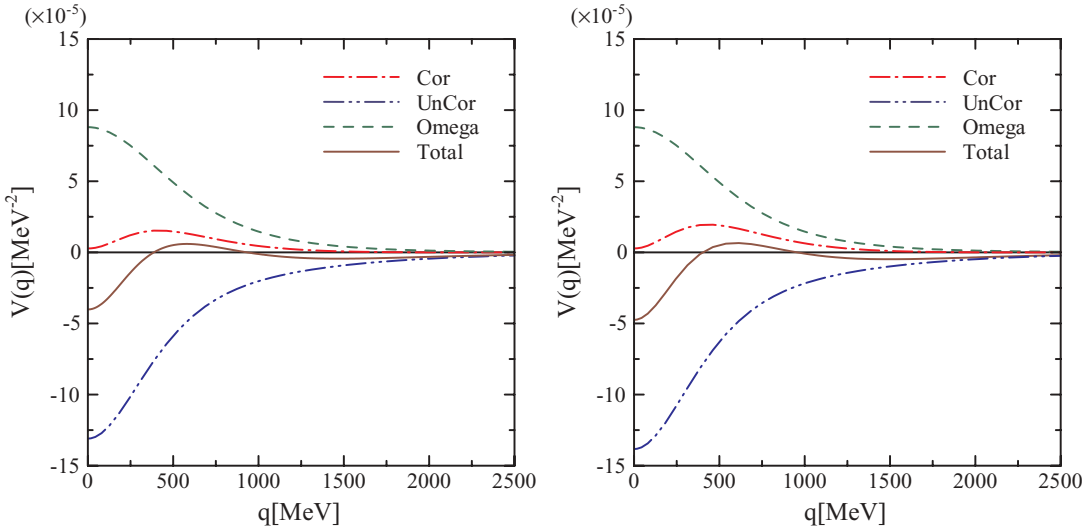

FIG. 9. (Color online) The scalar-isoscalar ΛN potential in momentum space with exchange of the pion pair (left) and with exchange of pion and kaon pairs (right).

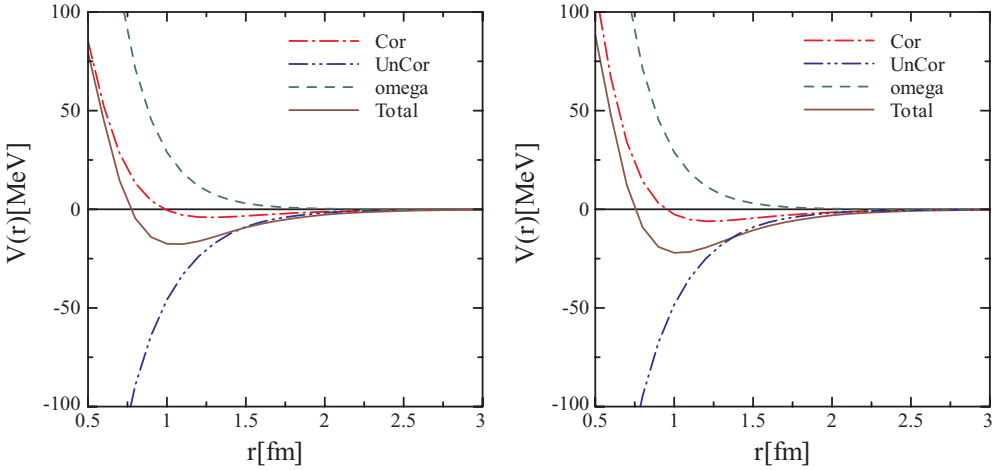

FIG. 10. (Color online) The scalar-isoscalar ΛN potential in configuration space with exchange of the pion pair (left) and with exchange of pion and kaon pairs (right).

$r \simeq 1.3$ fm. This potential is repulsive in the short-range region but is attractive beyond 1fm. As we have discussed in Sec. VII A, the strength of the correlated two-meson potential is much smaller than that of the other contributions.

Figure 10 also shows that the uncorrelated two-meson generates a strong attraction and the ω produces a repulsion in the short-range region. The sum of these two potentials produces a relatively strong attraction around 1fm and leads to large cancelations in the short-range region. We do not give the results below 0.5 fm since there the overlap of the baryons and quark exchange mechanisms can lead to sizable corrections.

Although the attraction in the total potential is mainly generated by the uncorrelated two-meson potential, part of the repulsion is generated by the correlated two-meson potential. This is interesting because the correlated two-meson potential is considered as a σ meson exchange in other papers and, there, the interaction would be always attractive (see Eq. (3.19) of [23]).

Here, again, we can check the effect of the two-kaon exchange potential by comparing the two panels in Fig. 10. The two-kaon contribution slightly enhances the magnitude of both the correlated and uncorrelated two-meson potential, and it makes the total potential a little deeper than the pionic potential.

C. The κ exchange ΛN potential

Figure 11 shows the κ exchange contribution in the ΛN potential. The potential in momentum space is shown in the left panel of Fig. 11. The correlated two-meson contribution has a shape similar to that of the scalar-isoscalar channel, but its size is an order of magnitude smaller.

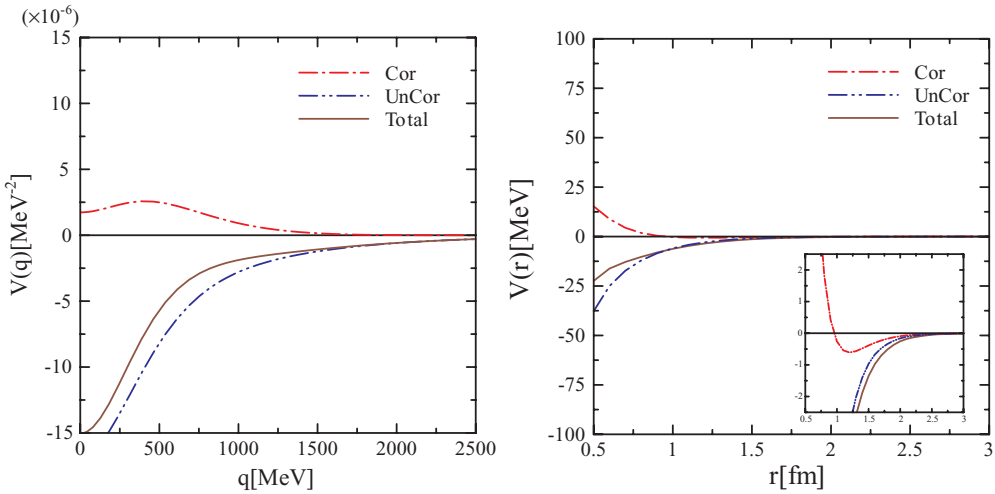

FIG. 11. (Color online) The ΛN potential in the κ channel for momentum space and configuration space. In the inset, we change the scale of the $V(r)$ axis to investigate the behavior of this potential.

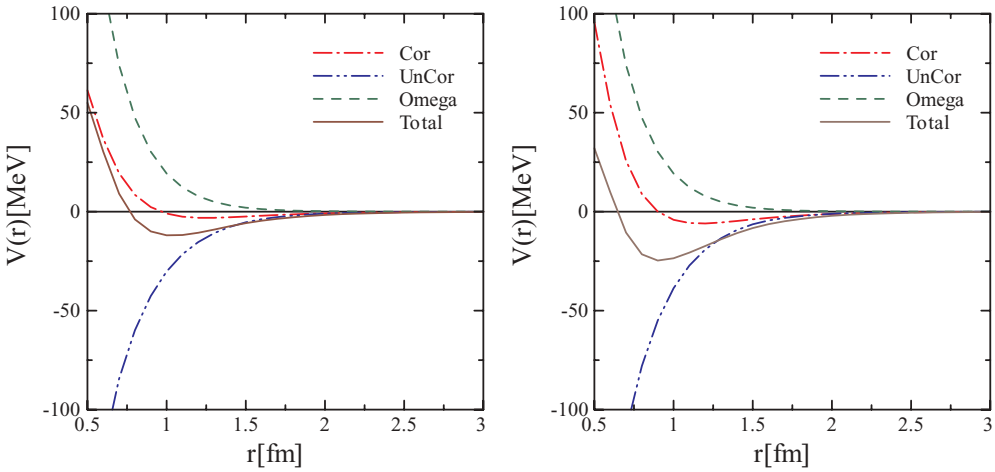

FIG. 12. (Color online) The scalar-isoscalar $\Lambda\Lambda$ potential in configuration space with exchange of the pion pair (left) and with exchange of pion and kaon pairs (right).

The uncorrelated two-meson exchange contribution generates an attraction that is relatively large compared to that of the correlated two-meson potential.

The right panel of Fig. 11 shows the potential in configuration space. The correlated two-meson contribution produces a moderate repulsion in the short-range region out to around 1.0 fm. The uncorrelated two-meson potential produces a weak attraction up to 2.0 fm. Both potentials are of a quite short range compared to the isoscalar channel. This reflects the heavy mass of the κ meson.

The total κ channel interaction is weakly attractive and of quite short range. The strength of the potential is weaker than the isoscalar potential, being almost one-third that at 1fm.

D. The $\Lambda\Lambda$ potential

Figure 12 shows the central part of the $\Lambda\Lambda$ potential. Both the uncorrelated two-meson and the ω exchange contribution are weaker than for the ΛN case, but they still have much larger magnitude than the correlated two-meson potential. These potentials drive the medium-range attraction. However, the ω exchange potential alone is not enough to produce a repulsion at shorter distances.

We find again that the correlated two-meson potential plays a dual role in making a repulsive potential in the short-range region and a small attraction in the long-range region. These properties are seen both in the left- and right-panel cases. The striking difference from the ΛN interaction is the large effect produced by the two-kaon exchange contribution. Both the correlated and uncorrelated two-meson potentials are largely enhanced by the two-kaon exchange diagrams, especially in the shorter range region. This effect leads to a large reduction of the short-range repulsion. Consequently, the short-range repulsion in the $\Lambda\Lambda$ potential is largely suppressed compared to the contribution of the two-pion exchange case and therefore to the NN or ΛN interaction where the $K\overline{K}$ exchange effect is much weaker.

TABLE I. Particle assignment for baryons and mesons.

Decuplet baryons	$T^{111}=\Delta^{++}$	$T^{112}=\frac{\Delta^{+}}{\sqrt{3}}$	$T^{122}=\frac{\Delta^{0}}{\sqrt{3}}$	$T^{222}=\Delta^{-}$
	$T^{113}=\frac{\Sigma^{*+}}{\sqrt{3}}$	$T^{123}=\frac{\Sigma^{*0}}{\sqrt{6}}$	$T^{223}=\frac{\Sigma^{*-}}{\sqrt{3}}$	
	$T^{133}=\frac{\Xi^{*0}}{\sqrt{3}}$	$T^{123}=\frac{\Xi^{*-}}{\sqrt{3}}$		
	$T^{333}=\Omega^{-}$			
Octet baryons	$B^1_{\bar{1}}=\frac{1}{\sqrt{6}}\Lambda+\frac{1}{\sqrt{2}}\Sigma^0$	$B^1_{\bar{2}}=\Sigma^+$	$B^1_{\bar{3}}=p$	
	$B^2_{\bar{1}}=\Sigma^-$	$B^2_{\bar{2}}=\frac{1}{\sqrt{6}}\Lambda-\frac{1}{\sqrt{2}}\Sigma^0$	$B^2_{\bar{3}}=n$	
	$B^3_{\bar{1}}=\Xi^-$	$B^3_{\bar{2}}=\Xi^0$	$B^3_{\bar{3}}=-\sqrt{\frac{2}{3}}\Lambda$	
Octet mesons	$\Phi^1_{\bar{1}}=\frac{1}{\sqrt{6}}\eta+\frac{1}{\sqrt{2}}\pi^0$	$\Phi^1_{\bar{2}}=\pi^+$	$\Phi^1_{\bar{3}}=K^+$	
	$\Phi^2_{\bar{1}}=\pi^-$	$\Phi^2_{\bar{2}}=\frac{1}{\sqrt{6}}\eta-\frac{1}{\sqrt{2}}\pi^0$	$\Phi^2_{\bar{3}}=K^0$	
	$\Phi^3_{\bar{1}}=\overline{K}^-$	$\Phi^3_{\bar{2}}=\overline{K}^0$	$\Phi^3_{\bar{3}}=-\sqrt{\frac{2}{3}}\eta$	

TABLE II. The α, β and γ coefficients of meson-baryon couplings.

$p \to$	$p\pi^0$	$n\pi^+$	ΛK^+	$\Sigma^0 K^+$	$\Sigma^+ K^0$		
α_{MBp}	1	$\sqrt{2}$	$-\frac{2}{\sqrt{3}}$	0	0		
β_{MBp}	0	0	$\frac{1}{\sqrt{3}}$	1	$\sqrt{2}$		
$p \to$	$\Delta^{++}\pi^-$	$\Delta^+\pi^0$	$\Delta^0\pi^+$	$\Sigma^{*+}K^0$	$\Sigma^{*0}K^+$		
γ_{MBp}	1	$-\sqrt{\frac{2}{3}}$	$-\frac{1}{\sqrt{3}}$	$\frac{1}{\sqrt{3}}$	$-\frac{1}{\sqrt{6}}$		
$n \to$	$p\pi^-$	$n\pi^0$	ΛK^0	$\Sigma^0 K^0$	$\Sigma^- K^+$		
α_{MBn}	$\sqrt{2}$	-1	$-\frac{2}{\sqrt{3}}$	0	0		
β_{MBn}	0	0	$\frac{1}{\sqrt{3}}$	-1	$\sqrt{2}$		
$n \to$	$\Delta^+\pi^-$	$\Delta^0\pi^0$	$\Delta^-\pi^+$	$\Sigma^{*0}K^0$	$\Sigma^{*-}K^+$		
γ_{MBn}	$\frac{1}{\sqrt{3}}$	$-\sqrt{\frac{2}{3}}$	-1	$\frac{1}{\sqrt{6}}$	$-\frac{1}{\sqrt{3}}$		
$\Lambda \to$	$\Sigma^+\pi^-$	$\Sigma^0\pi^0$	$\Sigma^-\pi^+$	pK^-	$n\overline{K}^0$	$\Xi^0 K^0$	$\Xi^- K^+$
$\alpha_{MB\Lambda}$	$\frac{1}{\sqrt{3}}$	$\frac{1}{\sqrt{3}}$	$\frac{1}{\sqrt{3}}$	$-\frac{2}{\sqrt{3}}$	$-\frac{2}{\sqrt{3}}$	$\frac{1}{\sqrt{3}}$	$\frac{1}{\sqrt{3}}$
$\beta_{MB\Lambda}$	$\frac{1}{\sqrt{3}}$	$\frac{1}{\sqrt{3}}$	$\frac{1}{\sqrt{3}}$	$\frac{1}{\sqrt{3}}$	$\frac{1}{\sqrt{3}}$	$-\frac{2}{\sqrt{3}}$	$-\frac{2}{\sqrt{3}}$
$\Lambda \to$	$\Sigma^{*+}\pi^-$	$\Sigma^{*0}\pi^0$	$\Sigma^{*-}\pi^+$	$\Xi^{*0}K^0$	$\Xi^{*-}K^+$		
$\gamma_{MB\Lambda}$	$-\frac{1}{\sqrt{2}}$	$\frac{1}{\sqrt{2}}$	$\frac{1}{\sqrt{2}}$	$-\frac{1}{\sqrt{2}}$	$\frac{1}{\sqrt{2}}$		

VIII. CONCLUSIONS

We have evaluated the scalar channel potential between the Λ and the nucleon. We have considered the correlated and uncorrelated two-meson exchange contributions in this channel in addition to the ω exchange. The correlated two-meson exchange contribution was calculated by using a chiral unitary approach, which reproduces very well the experimental meson-meson phase shift up to 1.2 GeV.

The uncorrelated two-meson exchange contribution produces a strong attraction, which is similar to the *NN* case. The ω exchange contribution comprises a short-range repulsion, also similar to the *NN* case, but its strength is two-thirds that of the *NN* case owing to the simple counting of nonstrange quarks in the baryons. These two contributions drive the attractive potential in the medium-range region and almost cancel each other at shorter distances.

The correlated two-meson exchange contribution is relatively smaller than the other two contributions. This potential produces some attraction at medium range and some strong repulsion in the short-range region. This behavior is quite similar to the *NN* case, which has already been calculated in [23]. The striking effect is the repulsion in the short-range region where the strong attraction generated by the uncorrelated two-meson potential is canceled by the repulsion produced by the ω meson. Thus the correlated two-meson potential plays an important role for both medium-range attraction and short-range repulsion in ΛN and $\Lambda\Lambda$ interactions.

We have also checked the contribution of two-kaon exchange diagrams. We have found that the two-kaon contribution is rather weak and it slightly enhances the magnitude of the potential without changing its main behavior for the ΛN potential. Therefore it does not play an important role in the scalar ΛN potential. However, it makes a large contribution to the $\Lambda\Lambda$ potential, especially in the short-distance region. It largely enhances both the repulsion in the correlated two-meson exchange potential and the attraction in the uncorrelated one. As a result, the total potential in the $\Lambda\Lambda$ interaction becomes more attractive than for the ΛN case and the short-range repulsion is also reduced.

We have also investigated the πK exchange in the κ channel for the case of the ΛN interaction and it shows similar features to those of the scalar isoscalar potential for a shorter range and sizably weaker strength.

Finally, we have found that the medium-range attraction and short-range repulsion largely depend on the flavor of the baryons. This flavor dependence of the central potential between baryons could be a clue to understanding certain properties of nuclear structure and reactions.

ACKNOWLEDGMENTS

One of us (K.S.) wishes to acknowledge support from the Ministerio de Educación y Ciencia and from the program of Estancias de Jóvenes Doctores y Tecnólogos Extranjeros en España. This work is partly supported by DGICYT Contract No. BFM2003-00856, and the E.U. EURIDICE network Contract No. HPRN-CT-2002-00311. This research is part of the EU Integrated Infrastructure Initiative Hadron Physics Project under Contract No. RII3-CT-2004-506078.

APPENDIX

After a nonrelativistic reduction is performed, the meson-baryon-baryon interaction with an emitted meson of momentum $\vec{q}$ is given by

$$-it^{\mathrm{Oct}} = \left(\alpha_{MBB'}\frac{D+F}{2f_\pi} + \beta_{MBB'}\frac{D-F}{2f_\pi}\right)\vec{\sigma}\cdot\vec{q}, \quad \text{(A1)}$$

$$-it^{\mathrm{Dec}} = \gamma_{MBB'}\frac{f^*_{\pi N\Delta}}{m_\pi}\vec{S}^\dagger\cdot\vec{q}, \quad \text{(A2)}$$

where the σ and S are spin transition operators for the octet-octet and the octet-decuplet cases. Here we define the $B \to B'M$ process with the particle assignment in Table I. The coefficients α, β and γ are listed in Table II.

[1] N. Hoshizaki, I. Lin, and S. Machida, Prog. Theor. Phys. **26**, 680 (1961); N. Hoshizaki, S. Otsuki, W. Watari, and M. Yonezawa, *ibid*. **27**, 1199 (1962).

[2] R. Machleidt, K. Holinde, and C. Elster, Phys. Rep. **149**, 1 (1987).

[3] J. S. Schwinger, Phys. Rev. D **3**, 1967 (1971).

[4] J. Binstock and R. Bryan, Phys. Rev. D **4**, 1341 (1971).
[5] M. M. Nagels, T. A. Rijken, and J. J. de Swart, Phys. Rev. D **17**, 768 (1978).
[6] P. M. M. Maessen, T. A. Rijken, and J. J. de Swart, Phys. Rev. C **40**, 2226 (1989).
[7] S. Eidelman *et al*. (Particle Data Group), Phys. Lett. **B592**, 1 (2004).
[8] See article of N. A. Tornqvist, in Ref. [7], p. 506.
[9] J. Gasser and U. G. Meissner, Nucl. Phys. **B357**, 90 (1991).
[10] U. G. Meissner, Comments Nucl. Part. Phys. **20**, 119 (1991).
[11] A. Dobado, M. J. Herrero, and T. N. Truong, Phys. Lett. **B235**, 134 (1990).
[12] A. Dobado and J. R. Pelaez, Phys. Rev. D **47**, 4883 (1993).
[13] J. A. Oller and E. Oset, Nucl. Phys. **A652**, 438 (1997); **A652**, 407(E) (1999).
[14] J. A. Oller, E. Oset, and J. R. Pelaez, Phys. Rev. D **59**, 074001 (1999); **60**, 099906(E) (1999).
[15] J. A. Oller and E. Oset, Phys. Rev. D **60**, 074023 (1999).
[16] N. Kaiser, Eur. Phys. J. A **3**, 307 (1998).
[17] V. E. Markushin, Eur. Phys. J. A **8**, 389 (2000).
[18] J. Nieves and E. Ruiz Arriola, Phys. Lett. **B455**, 30 (1999).
[19] F. K. Guo, R. G. Ping, P. N. Shen, H. C. Chiang, and B. S. Zou, Nucl. Phys. **A773**, 78 (2006).
[20] N. A. Tornqvist and M. Roos, Phys. Rev. Lett. **76**, 1575 (1996).
[21] E. Van Beveren, T. A. Rijken, K. Metzger, C. Dullemond, G. Rupp, and J. E. Ribeiro, Z. Phys. C **30**, 615 (1986).
[22] E. van Beveren and G. Rupp, Eur. Phys. J. C **22**, 493 (2001).
[23] E. Oset, H. Toki, M. Mizobe, and T. T. Takahashi, Prog. Theor. Phys. **103**, 351 (2000).
[24] N. Kaiser, S. Gerstendorfer, and W. Weise, Nucl. Phys. **A637**, 395 (1998).
[25] J. F. Donoghue, w arXiv:nucl-th/0602074.
[26] D. Jido, E. Oset, and J. E. Palomar, Nucl. Phys. **A694**, 525 (2001).
[27] R. B. Wiringa, R. A. Smith, and T. L. Ainsworth, Phys. Rev. C **29**, 1207 (1984).
[28] R. B. Wiringa, V. G. J. Stoks, and R. Schiavilla, Phys. Rev. C **51**, 38 (1995).
[29] V. G. J. Stoks and T. A. Rijken, Phys. Rev. C **59**, 3009 (1999).
[30] T. A. Rijken, V. G. J. Stoks, and Y. Yamamoto, Phys. Rev. C **59**, 21 (1999).
[31] T. A. Rijken and Y. Yamamoto, Phys. Rev. C **73**, 044008 (2006).
[32] K. Tominaga and T. Ueda, Nucl. Phys. **A693**, 731 (2001).
[33] U. Straub, Z. Y. Zhang, K. Brauer, A. Faessler, S. B. Khadkikar, and G. Lubeck, Nucl. Phys. **A483**, 686 (1988).
[34] Z. Y. Zhang, A. Faessler, U. Straub, and L. Y. Glozman, Nucl. Phys. **A578** 573 (1994).
[35] Z. Y. Zhang, Y. W. Yu, P. N. Shen, L. R. Dai, A. Faessler, and U. Straub, Nucl. Phys. **A625**, 59 (1997).
[36] Y. Fujiwara, C. Nakamoto, Y. Suzuki, M. Kohno, and K. Miyagawa, Prog. Theor. Phys. Suppl. **156**, 17 (2004).
[37] J. Haidenbauer and U.-G. Meissner, Phys. Rev. C **72**, 044005 (2005).
[38] B. Holzenkamp, K. Holinde, and J. Speth, Nucl. Phys. **A500**, 485 (1989).
[39] A. Reuber, K. Holinde, and J. Speth, Nucl. Phys. **A570**, 543 (1994).
[40] J. Gasser and H. Leutwyler, Nucl. Phys. **B250**, 465 (1985).
[41] J. Gasser and H. Leutwyler, Nucl. Phys. **B250**, 517 (1985).
[42] J. Gasser and H. Leutwyler, Nucl. Phys. **B250**, 539 (1985).
[43] G. Ecker, Prog. Part. Nucl. Phys. **35**, 1 (1995).
[44] U. G. Meissner, Rep. Prog. Phys. **56**, 903 (1993).
[45] V. Bernard, N. Kaiser, and U. G. Meissner, Int. J. Mod. Phys. E **4**, 193 (1995).
[46] J. A. Oller, E. Oset, and A. Ramos, Prog. Part. Nucl. Phys. **45**, 157 (2000).
[47] S. N. Cherry and M. R. Pennington, Nucl. Phys. **A688**, 823 (2001).
[48] D. V. Bugg, Eur. Phys. J. C **47**, 57 (2006).
[49] Z. Y. Zhou and H. Q. Zheng, Nucl. Phys. **A775**, 212 (2006).
[50] D. V. Bugg, Phys. Lett. **B632**, 471 (2006).
[51] M. Ablikim *et al*. (BES Collaboration), Phys. Lett. **B633**, 681 (2006).
[52] F. J. Llanes-Estrada, E. Oset, and V. Mateu, Phys. Rev. C **69**, 055203 (2004).
[53] M. M. Kaskulov, E. Oset, and M. J. Vicente Vacas, Phys. Rev. C **73**, 014004 (2006).